



**Amorphous Titanic Acid Electrode: Its Electrochemical Storage of Ammonium in a New Water-in-Salt Electrolyte**

Journal:	<i>ChemComm</i>
Manuscript ID	CC-COM-06-2018-004713.R1
Article Type:	Communication

SCHOLARONE™  
Manuscripts



ChemComm

COMMUNICATION

## Amorphous Titanic Acid Electrode: Its Electrochemical Storage of Ammonium in a New Water-in-Salt Electrolyte

Received 00th January 20xx,  
Accepted 00th January 20xx

John J. Holoubek, Heng Jiang, Daniel Leonard, Yitong Qi, Galo C. Bustamante, Xiulei Ji\*

DOI: 10.1039/x0xx00000x

www.rsc.org/

**We report an amorphous titanic acid of  $\text{TiO}_{1.85}(\text{OH})_{0.30} \cdot 0.28\text{H}_2\text{O}$  as a new electrode for aqueous ammonium-ion batteries, which operates in a new water-in-salt electrolyte—25 m  $\text{NH}_4\text{CH}_3\text{COO}$ . The titanic acid electrode exhibits a specific capacity nearly 8 times that from the crystalline  $\text{TiO}_2$  electrode. In electrochemical reactions, the amorphous titanic acid provides abundant storage sites in its disordered structure and affords strong H-bonding toward the inserted  $\text{NH}_4^+$  ions.**

To enable wide utilization of renewable energy, i.e., wind and solar, stationary storage solutions are the missing enablers, where electrochemical energy storage (EES) systems should play a critical role. Considering safety, EES devices utilizing non-flammable aqueous electrolytes are particularly promising. For aqueous EES, the electrolyte potential window that only spans 1.23 V thermodynamically has been widened up to 3 V via extremely concentrated aqueous electrolytes, known as “Water-in-Salt” electrolytes (WiSE), e.g., lithium bis(trifluoromethane)sulfonimide (LiTFSI).<sup>1</sup> In WiSE the fewer water molecules available are tightly bound in the primary solvation sheath of electrolyte ions. This reduced solvation number decreases the HOMO level of water, which renders water splitting reactions more difficult, particularly, the oxygen evolution reaction (OER), and the lower activity of water would also ‘delay’ its splitting reactions, including the hydrogen evolution reaction (HER) according to the Nernst equation.<sup>1–3</sup> In addition, anions in WiSE, e.g., TFSI, are more reactive by having a lower LUMO, thus readily forming the solid electrolyte interphase (SEI) on anodes, which further expands water’s electrochemical stability window.<sup>1,2,4</sup> This not only promises higher energy densities of aqueous batteries, but more importantly engenders the development of new electrode materials that were previously deemed unusable in aqueous systems, such as materials with the  $\text{Ti}^{4+}/\text{Ti}^{3+}$  redox couple.<sup>5–8</sup>

Among materials that could use the  $\text{Ti}^{4+}/\text{Ti}^{3+}$  redox couple, there exist a class of “titanic acids” with a general formula of  $\text{TiO}_x(\text{OH})_{4-2x}$ , which exhibit a variety of structures.<sup>9,10</sup> In fact, titanic acids have been widely employed as precursors for the  $\text{TiO}_2$  synthesis,<sup>11–13</sup> ion exchange/absorption,<sup>14,15</sup> and catalysis.<sup>16,17</sup> It was not until very recently that titanic acids have demonstrated relevance in battery tests, where it was aimed to utilize the abundant structural defects in them to achieve a high capacity.<sup>18,19</sup> However, the operation potentials of titanic acids are often too low to exhibit reversible ion storage properties in aqueous electrolytes.

Recently, the concept of WiSE has been furthered from lithium-based electrolytes to ones that are based on earth-abundant metal cations, such as  $\text{NaFSI}^5$ , and  $\text{Zn}(\text{CF}_3\text{SO}_3)_2$ .<sup>20</sup> To date, most reported WiSE utilize expensive fluorinated salts except for 30 m  $\text{KCH}_3\text{COO}$  (KAc).<sup>7,21</sup>

In batteries, the choice of ion charge carriers essentially defines the properties of devices. Despite the debuts of nearly all relevant metal ions, nonmetal ions such as proton, hydronium, and ammonium have received little attention although these ions may offer rich binding chemistry with electrodes.<sup>22</sup>

To explore the potential of WiSE based on non-metal cations, herein, we demonstrate an aqueous solution of 25 m  $\text{NH}_4\text{CH}_3\text{COO}$  (AmAc) as the electrolyte, in which a titanic acid of  $\text{TiO}_{1.85}(\text{OH})_{0.30} \cdot 0.28\text{H}_2\text{O}$  exhibits an ammonium storage capacity nearly 8 times that of the crystalline  $\text{TiO}_2$ . As one distinct factor, we observed the evidence of strong hydrogen bonding of the stored  $\text{NH}_4^+$  within the titanic acid electrode but not with crystalline  $\text{TiO}_2$  electrode. In addition, titanic acid has a lower density, a higher surface area, and a defect-rich amorphous structure, which may relate to the performance disparity between the two electrode materials as well.

We prepared the amorphous titanic acid and  $\text{TiO}_2$  by a facile sol-gel method at room temperature (see Supporting Information), where their preparation only differs in the final annealing temperature for the sol-gel precipitate—110 °C and

Department of Chemistry, Oregon State University, Corvallis, Oregon, United States, 97331 E-mail: david.ji@oregonstate.edu

Electronic Supplementary Information (ESI) available: Experimental details of syntheses, materials characterization, and electrochemical measurement as well as TGA, SEM, BET, electrolyte conductivity, FTIR, and additional CV data.

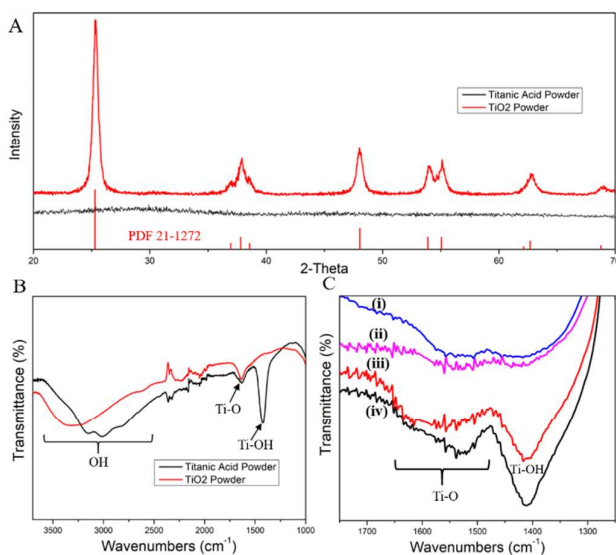


**Figure 1.** (A) Powder XRD patterns of the titanic acid and  $\text{TiO}_2$ . FTIR spectra of (B) pristine titanic acid, and  $\text{TiO}_2$  powder, (C) (i) pristine  $\text{TiO}_2$  electrode, (ii) ammoniated  $\text{TiO}_2$  electrode, (iii) pristine titanic acid electrode, and (iv) ammoniated titanic acid electrode.

450 °C for titanic acid and  $\text{TiO}_2$ , respectively. Thermogravimetric analysis (TGA) of titanic acid reveals mass loss of 9.7% from 50 - 450 °C in a distinct three-slope profile (**Fig. S1A**), where we attribute to removal of physisorbed water, lattice water, and the conversion from  $\text{TiO}_x(\text{OH})_{4-2x}$  to  $\text{TiO}_2 + (2-x)\text{H}_2\text{O}$ . The formula of the titanic acid is, thus, determined to be  $\text{TiO}_{1.85}(\text{OH})_{0.30} \cdot 0.28\text{H}_2\text{O}$ .

The  $\text{TiO}_2$  formed at 450 °C exhibits a highly crystalline anatase structure, whereas the titanic acid is completely amorphous, as revealed by their X-ray diffraction (XRD) patterns (**Figure 1A**). Scanning electron microscopy (SEM) imaging of the titanic acid shows large variance of particle sizes (**Figure S1B, C**). The hysteresis of the  $\text{N}_2$  sorption isotherms of the titanic acid is characteristic of a mesoporous structure, where it exhibits the specific Brunauer–Emmett–Teller (BET) surface area of 214  $\text{m}^2/\text{g}$  and the pores size distribution (PSD) under 10 nm (**Figure S2A, B**). The  $\text{TiO}_2$  has a BET surface area of 80  $\text{m}^2/\text{g}$  and the PSD from 10 to 60 nm (**Figure S2C, D**).

In Fourier transform infrared spectroscopy (FTIR), both titanic acid and  $\text{TiO}_2$  display the vibration of the Ti-O bond at 1700  $\text{cm}^{-1}$ , and titanic acid shows a peak of Ti-OH bond at 1400  $\text{cm}^{-1}$  (**Figure 1B**).<sup>23</sup> Instead of having a single peak at 3300  $\text{cm}^{-1}$  assigned to the surface adsorbed water on the  $\text{TiO}_2$  particles, titanic acid exhibits multiple peaks for O-H vibrations near 3000  $\text{cm}^{-1}$ , which indicates the existence of crystal water molecules and hydroxide groups inside the titanic acid in addition to the physisorbed water.

The electrochemical performance of all samples was evaluated in three-electrode cells using a free-standing film of activated carbon (AC) as the counter electrode and an Ag/AgCl reference electrode. Aluminum and titanium rods were used as anode and cathode current collectors, respectively, to provide a

wide electrochemical stability window.<sup>2,24</sup> As shown in **Figure 2A**, the 25 m AmAc electrolyte shows a potential window of 2.95 V in contrast to 2.25 V of the 1 M counterpart. Much of its wider range comes from the greater anodic stability characteristics. However, as observed in previous works electrolytes' concentration has little effect on water's cathodic stability.<sup>2,25</sup> In fact, the 25 m AmAc electrolyte is slightly less stable cathodically than the 1 M AmAc on the bare surface of Al current collector despite having a higher pH value of 7.7, in contrast to 1 M AmAc, which exhibits a pH of 6.9. This phenomenon is likely due to the mechanism:  $2\text{NH}_4^+ + 2\text{e}^- \rightarrow 2\text{NH}_3 + \text{H}_2$  based on the Le Chatelier principle. This phenomenon was previously observed when increasing  $\text{NH}_4^+$  concentration at a constant pH value.<sup>26</sup> However, it is worth noting that when the titanic acid electrode is coated onto the Al current collector less HER occurs in 25 m AmAc than in 1 M AmAc, as displayed in **Figure 2B**, opposite to the stability trend observed on the blank Al electrode. Recently, it has been observed that when a WiSE is used, it typically raises the operation potential of its cation-insertion electrode due to the increased activity of the cations.<sup>2</sup> In this case, the reduction potential for the titanic acid becomes higher in WiSE than in a dilute electrolyte. Thus, in WiSE, the titanic acid electrode gets reduced before the  $\text{NH}_4^+$  ions do, and the HER behavior on the titanic acid in WiSE looks mitigated.

The titanic acid electrode exhibits a galvanostatic charge-discharge (GCD) specific capacity of 84  $\text{mAh g}^{-1}$  in the WiSE of 25 m AmAc and 61  $\text{mAh g}^{-1}$  in 1 M AmAc. These are much higher than the capacity of  $\text{TiO}_2$  — 11  $\text{mAh g}^{-1}$  (**Figure 3A, B**). Furthermore, the 25 m AmAc electrolyte provides a higher specific capacity for the titanic acid electrode than the 1 M AmAc at 1 A  $\text{g}^{-1}$ , which we believe is due to the increased redox potential of the titanic acid when tested in the WiSE, where at the same lower cutoff potential, more capacity could be released.

It is worth noting that there are slightly larger current and more charges in the cathodic process than the anodic process in CV and GCD measurements, which we believe is due to HER. This may cause the consumption of the aqueous electrolyte during cycling and lead to the potential failure of the full cells in long cycling.

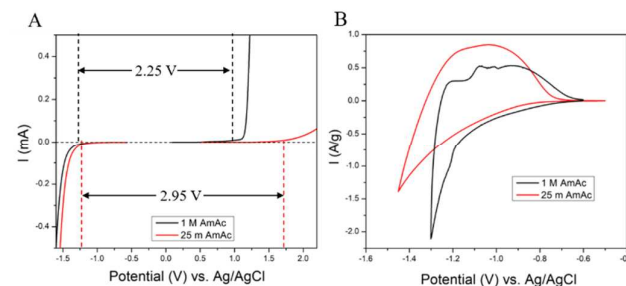


**Figure 2.** (A) Cyclic voltammetry (CV) curves recorded in 1 M and 25 m AmAc electrolytes at 1  $\text{mV s}^{-1}$ . Onset potentials were selected when the current is 0.01 mA. (B) CV curves of the titanic acid electrode in 1 M and 25 m AmAc electrolytes at 1  $\text{mV s}^{-1}$ .

To understand the capacity disparity between the titanic acid and  $\text{TiO}_2$ , we first measured the density of titanic acid and  $\text{TiO}_2$  by the Archimedes principle as  $2.41 \text{ g cm}^{-3}$  and  $3.00 \text{ g cm}^{-3}$ , respectively. The results suggest there are more available sites for  $\text{NH}_4^+$  storage in the titanic acid's structure. Another aspect accounting for the capacity difference may arise from the abundant defects in the amorphous structure of the titanic acid for binding  $\text{NH}_4^+$ .<sup>18</sup> This trend is widely observed in the capacity difference among the storage of  $\text{Li}^+$ ,  $\text{Na}^+$ , and  $\text{K}^+$  ions.<sup>19</sup>

As another critical point,  $\text{NH}_4^+$  forms very strong chemical bonds with local groups in the titanic acid but not with  $\text{TiO}_2$ . We employed *ex situ* FTIR spectroscopy to investigate pristine and ammoniated titanic acid and  $\text{TiO}_2$  free-standing film electrodes. **Figure 1C** displays the broad Ti-O bond peak from  $1550$  to  $1600 \text{ cm}^{-1}$ , which undergoes a significant red-shift after the ammoniation of the titanic acid at  $-1.3 \text{ V}$  vs.  $\text{Ag}/\text{AgCl}$ . This red-shift of the peak indicates that the Ti-O bond is weakened due to the interaction via the  $\text{NH}_4^+$ -O-Ti hydrogen bond. For the  $\text{TiO}_2$  electrode, ammoniation does not cause a significant peak shift, which certainly relates to the small storage capacity but also to the lack of a chemical environment in  $\text{TiO}_2$  for hydrogen bonding.

Furthermore, the titanic acid electrode also exhibits good rate performance, exhibiting a reversible storage capacity of  $70 \text{ mAh g}^{-1}$  and  $50 \text{ mAh g}^{-1}$  in  $25 \text{ m}$  and  $1 \text{ M}$  AmAc, respectively, at  $5 \text{ A g}^{-1}$  (**Figure 3C** and **D**). Additionally, the  $25 \text{ m}$  AmAc displays a higher capacitive nature of the storage, measured to be  $79.1\%$ , where it was  $52.3\%$  for the  $1 \text{ M}$  AmAc system (**Figure S5A, B**).

Note that there is a lack of conductivity disparity between  $25 \text{ m}$  and  $1 \text{ M}$  AmAc (**Figure S3A**). **Figure 3E** and **3F** show that the titanic acid electrode in the  $25 \text{ m}$  AmAc electrolyte retains  $80\%$  capacity after 125 cycles, whereas in  $1 \text{ M}$  AmAc its CE deteriorates rapidly despite exhibiting less capacity decay.

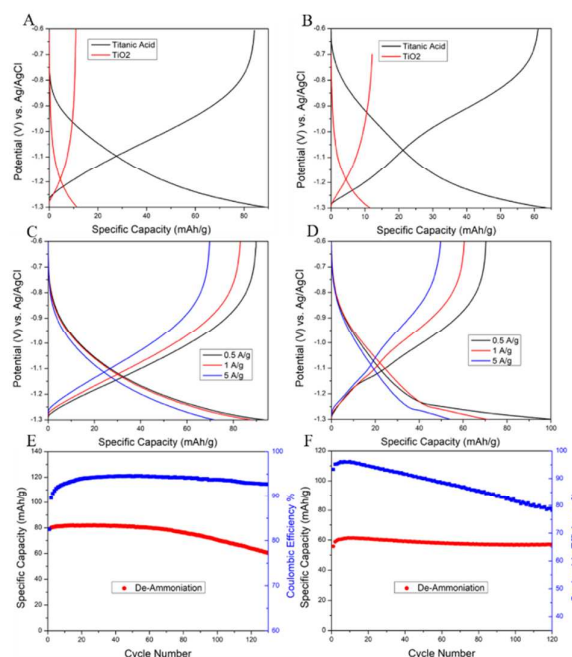


**Figure 3.** Typical GCD profiles of the titanic acid and  $\text{TiO}_2$  electrodes at  $1 \text{ A g}^{-1}$  in (A)  $25 \text{ m}$  AmAc, (B)  $1 \text{ M}$  AmAc. Rate performance of the titanic acid electrode at various specific current in (C)  $25 \text{ m}$  AmAc, (D)  $1 \text{ M}$  AmAc. Cycling performance of the titanic acid electrode at  $1 \text{ A g}^{-1}$  in (E)  $25 \text{ m}$  AmAc, (F)  $1 \text{ M}$  AmAc.

This indicates that in the  $1 \text{ M}$  AmAc HER dominates, corroborating the observed stability trend in **Figure 2B**, and further demonstrates the advantage of AmAc WiSE over the dilute electrolytes. The slightly faster fading in  $25 \text{ m}$  AmAc is not well understood at this stage.

In summary, an amorphous titanic acid with the formula of  $\text{TiO}_{1.85}(\text{OH})_{0.30} \cdot 0.28\text{H}_2\text{O}$  was synthesized through a facile sol-gel method. In the AmAc WiSE, the titanic acid electrode exhibits enhanced cathodic stability, delivers a higher specific capacity, and shows a greater capacitive contribution of ion storage compared to the case of the  $1 \text{ M}$  electrolyte. In addition, the titanic acid exhibits the capacity of  $\text{NH}_4^+$  storage nearly 8 times that of the crystalline  $\text{TiO}_2$  at the same conditions, where the higher capacity is attributed to the lower density of the titanic acid, its amorphous structure, and the strong hydrogen bonding between the hydroxide structure and the inserted  $\text{NH}_4^+$ . This work represents an addition to the aqueous energy storage by introducing one rarely known electrode material—titanic acid that accommodates  $\text{NH}_4^+$  in a new AmAc WiSE system that by itself may be interesting to various fields.

### Acknowledgements:

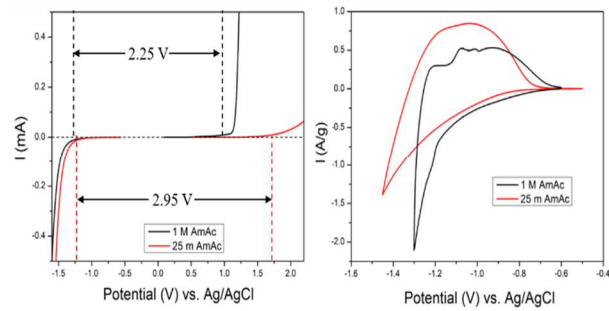
X. Ji thanks the financial supports from the National Science Foundation of the United States, Award Number: 1551693.

### Conflicts of interest

There are no conflicts to declare.

### Notes and references

- 1 L. Suo, O. Borodin, T. Gao, M. Olguin, J. Ho, X. Fan, C. Luo, C. Wang and K. Xu, *Science*, 2015, **350**, 938–943.
- 2 Y. Yamada, K. Usui, K. Sodeyama, S. Ko, Y. Tateyama and A. Yamada, *Nature Energy*, 2016, **1**, 16129.
- 3 J. O. Bockris and A. K. N. Reddy, *Volume 1: Modern Electrochemistry: Ionics*, Springer US, 2nd edn., 1998.
- 4 C. Yang, J. Chen, T. Qing, X. Fan, W. Sun, A. von Cresce, M. S. Ding, O. Borodin, J. Vatamanu, M. A. Schroeder, N. Eidson, C. Wang and K. Xu, *Joule*, 2017, **1**, 122–132.
- 5 R.-S. Kühnel, D. Reber and C. Battaglia, *ACS Energy Letters*, 2017, **2**, 2005–2006.
- 6 L. Suo, O. Borodin, W. Sun, X. Fan, C. Yang, F. Wang, T. Gao, Z. Ma, M. Schroeder, A. von Cresce, S. M. Russell, M. Armand, A. Angell, K. Xu and C. Wang, *Angewandte Chemie International Edition*, 2016, **55**, 7136–7141.
- 7 D. P. Leonard, Z. Wei, G. Chen, F. Du and X. Ji, *ACS Energy Letters*, 2018, 373–374.
- 8 F. Wang, O. Borodin, M. S. Ding, M. Gobet, J. Vatamanu, X. Fan, T. Gao, N. Edison, Y. Liang, W. Sun, S. Greenbaum, K. Xu and C. Wang, *Joule*, 2018, **2**, 927–937.
- 9 T. Sotokawa, N. Moriyama, M. Homma, United States Patent, US20110073804A1, 2011.
- 10 V. Legrand, O. Merdrignac-Conanec, W. Paulus and T. Hansen, *Journal of Physical Chemistry A*, 2012, **116**, 9561–9567.
- 11 Y.-J. Liu, M. Aizawa, Z.-M. Wang, H. Hatori, N. Uekawa and H. Kanoh, *Journal of Colloid and Interface Science*, 2008, **322**, 497–504.
- 12 N. Murakami, Y. Kurihara, T. Tsubota and T. Ohno, *Journal of Physical Chemistry C*, 2009, **113**, 3062–3069.
- 13 T. P. Feist and P. K. Davies, *Journal of Solid State Chemistry*, 1992, **101**, 275–295.
- 14 T. Wajima, Y. Umetsu, S. Narita and K. Sugawara, *Desalination*, 2009, **249**, 323–330.
- 15 T. Ishihara, Y. Misumi and H. Matsumoto, *Microporous and Mesoporous Materials*, 2009, **122**, 87–92.
- 16 X. Li, N. Kikugawa and J. Ye, *Chemistry A European Journal*, 2009, **15**, 3538–3545.
- 17 Y. Yuan, K. Asakura, A. P. Kozlova, H. Wan, K. Tsai and Y. Iwasawa, *Catalysis Today*, 1998, **44**, 333–342.
- 18 J. Ma, K. G. Reeves, A.-G. Porras Gutierrez, M. Body, C. Legein, K. Kakinuma, O. J. Borkiewicz, K. W. Chapman, H. Groult, M. Salanne and D. Dambournet, *Chemistry of Materials*, 2017, **29**, 8313–8324.
- 19 K. G. Reeves, J. Ma, M. Fukunishi, M. Salanne, S. Komaba and D. Dambournet, *ACS Applied Energy Materials*, 2018, **1**, 2078–2086.
- 20 P. Hu, M. Yan, T. Zhu, X. Wang, X. Wei, J. Li, L. Zhou, Z. Li, L. Chen and L. Mai, *ACS Applied Materials and Interfaces*, 2017, **9**, 42717–42722.
- 21 Z. Tian, W. Deng, X. Wang, C. Liu, C. Li, J. Chen, M. Xue, R. Li and F. Pan, *Functional Materials Letters*, 2017, **10**, 1750081.
- 22 X. Wu, Y. Qi, J. J. Hong, Z. Li, A. S. Hernandez and X. Ji, *Angewandte Chemie International Edition*, **56**, 13026–13030.
- 23 W. Low and V. Boonamnuayvitaya, *Materials Research Bulletin*, 2013, **48**, 2809–2816.
- 24 R.-S. Kühnel, D. Reber, A. Remhof, R. Figi, D. Bleiner and C. Battaglia, *Chemical Communications*, 2016, **52**, 10435–10438.
- 25 L. Coustan, G. Shul and D. Bélanger, *Electrochemistry Communications*, 2017, **77**, 89–92.
- 26 T. N. Andersen, B. S. Dandapani and J. M. Berry, *Journal of Electroanalytical Chemistry*, 1993, **357**, 77–89.
- 27 J. Wang, J. Polleux, J. Lim and B. Dunn, *Journal of Physical Chemistry C*, 2007, **111**, 14925–14931.
- 28 A. Zecchina, L. Marchese, S. Bordiga, C. Pazè and E. Gianotti, *Journal of Physical Chemistry B*, 1997, **101**, 10128–10135.
- 29 L. Suo, Y.-S. Hu, H. Li, M. Armand and L. Chen, *Nature Communications*, 2013, **4**, 1481.



Amorphous titanic acid reversibly stores  $\text{NH}_4^+$  in a new AmAc WiSE system.